ELECTRONIC DEFECTS AND INTERFACE POTENTIALS FOR Al OXIDE FILMS ON Al AND THEIR RELATIONSHIP TO ELECTROCHEMICAL PROPERTIES

J. P. Sullivan, R. G. Dunn, J. C. Barbour, F. D. Wall, N. Missert, and R. G. Buchheit*
Sandia National Laboratories, Albuquerque, NM 87185
*The Ohio State University, Columbus, OH 43210

ABSTRACT

The relative electronic defect densities and oxide interface potentials were determined for naturally-occurring and synthetic Al oxides on Al. In addition, the effect of electrochemical treatment on the oxide electrical properties was assessed. The measurements revealed (1) that the open circuit potential of Al in aqueous solution is inversely correlated with the oxide electronic defect density (viz., lower oxide conductivities are correlated with higher open circuit potentials), and (2) the electronic defect density within the Al oxide is increased upon exposure to an aqueous electrolyte at open circuit or applied cathodic potentials, while the electronic defect density is reduced upon exposure to slight anodic potentials in solution. This last result, combined with recent theoretical predictions, suggests that hydrogen may be associated with electronic defects within the Al oxide, and that this H may be a mobile species, diffusing as H^+. The potential drop across the oxide layer when immersed in solution at open circuit conditions was also estimated and found to be 0.3 V, with the field direction attracting positive charge towards the Al/oxide interface.

INTRODUCTION

The corrosion response and electrochemistry of pure Al in an aqueous electrolyte is normally governed by the nature and properties of the thin passivating Al oxide layer on the surface. The electrical properties and interface potentials of this oxide layer can play an important role in electrochemistry because electron transport across the oxide is necessary for supporting the oxidation and reduction reactions that occur at the metal and electrolyte interfaces of the oxide. In addition, the potentials at the oxide interfaces establish a field across the oxide which assists in the transport of charged species across the layer.

In this study, the electrical properties of thin, naturally-occurring and artificially grown and deposited Al oxide layers on Al were examined and then correlated with the electrochemical behavior of Al. Changes in the electrical properties of the oxide layer were also measured following electrochemical polarization of the sample in a non-aggressive electrolyte. The dielectric breakdown characteristics of the oxide and potential drop across the oxide were also evaluated. These results reveal that some of the electrochemical behavior of pure Al can be understood on the basis of the oxide electrical properties and that species, such as H, may be associated with important electrical and electrochemical characteristics of Al.

DISCLAIMER

EXPERIMENTAL

Solid state electrical measurements were performed using lithographically-patterned contacts of either Au or Al on to specially-prepared Al oxide layers on thin films of pure Al. The Al films, typically 0.15 to 0.2 μm thick, were thermally evaporated from 99.9999% pure Al at a base pressure of ~ 10^{-9} Torr on to SiO_2-coated Si substrates. The oxide layer was formed in the vacuum chamber immediately after Al deposition either by exposing the Al surface to pure $O_{2(g)}$ at 1 Torr for 90 min., oxidizing the sample in an electron cyclotron resonance (ECR) oxygen plasma for about 10 min., or depositing an Al_2O_3 layer in the ECR system using thermal evaporation of Al in an oxygen plasma. All of the oxides formed in these procedures are amorphous in structure with stoichiometry of Al_2O_3. The $O_{2(g)}$-formed oxides and ECR grown oxides grew to a thickness of about 4.5 nm, as determined by capacitance measurements, while the ECR deposited oxide layers were formed with thicknesses ranging from about 5 nm to over 20 nm, with deposition to a thickness of 10 nm being typical.

Electrical measurements were made in a metal-insulator-metal (MIM) configuration by electrically contacting the Al layer beneath the oxide and the top contact metal (either Al or Au). Typically, a square top contact of size 50 μm by 50 μm was used. The electrochemical measurements were performed in aerated 0.05 M K_2SO_4 solutions. Changes in the oxide electronic defect density were determined by measuring the oxide solid state electrical properties prior to and following electrochemical treatment. When the solid state electrical properties of the oxide were measured subsequent to electrochemical treatment, the sample was patterned with photoresist, leaving areas of exposed oxide, but the top metal contacts were not yet applied. The top metal contacts were deposited after the electrochemical processing by a process of thermal evaporation of the contact metal (either Au or Al) under high vacuum followed by lift-off of the contact metal in the photoresist-covered regions.

RESULTS AND DISCUSSION

The sections that follow discuss the measurement of electronic defects in Al oxide layers and how these defects influence electrochemical properties. It is then discussed how electrochemical treatment (e.g. anodic and cathodic polarization) modifies the electronic defect density of the Al oxide. Finally, the magnitude of the interfacial potentials and, more importantly, the electric field that is present in the oxide due to immersion of the sample in water are discussed.

Electronic Defects and Electrochemical Properties

Measurements of the current-voltage characteristics of the oxide layers indicate that the current conduction mechanism obeys Frenkel-Poole conduction which originates from field-assisted thermal emission of carriers from deep electron traps within the Al oxide layer, see Fig. 1 (1). For Frenkel-Poole conduction, the current across the oxide layer is given by

$$I = \frac{AC'V}{d}\exp\left[-\frac{q}{k_B T}\left(\Phi_B - \sqrt{\frac{qV}{\pi\varepsilon_i\varepsilon_0 d}}\right)\right], \qquad [1]$$

where A is the area of the contact, C' is the density of electronic traps, V is the applied voltage, d is the thickness of the oxide layer, T is the temperature, and Φ_B is the trap well depth (the height of the barrier – at zero applied field – that the carrier must surmount in order to escape the trap) (2). Within the same defect type, the trap well depth should be constant (or narrowly distributed due, for example, to variability in the local bonding environment), so that the magnitude of the observed current at constant voltage should be directly proportional to the electronic defect density within the oxide layer. Hence, current-voltage characterization becomes a convenient tool to assess relative electronic defect concentrations among different Al oxide layers.

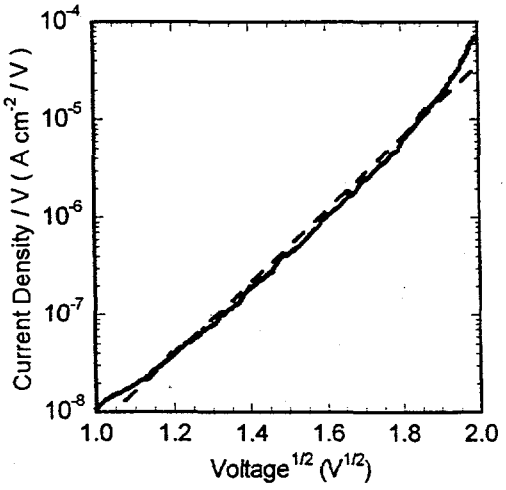

Fig. 1. Current-voltage characteristics for a 24 nm thick ECR deposited Al_2O_3 layer on Al. The dashed line is the predicted functional dependence for Frenkel-Poole conduction.

The three types of Al oxide layers (the O_2-formed, ECR plasma grown, and ECR deposited oxides) exhibit different conductivities and, assuming a common defect type for each sample, different electronic defect densities. This is readily apparent from the current-voltage characteristics of these layers, see Fig. 2. The sample which exhibits the highest leakage current is the O_2-formed oxide, while the sample with the lowest leakage current is the ECR deposited oxide. Although there are slight differences in thicknesses for the layers (4.5 nm for the O_2-formed and ECR grown oxide and 8.0 nm for this ECR deposited oxide), the differences in oxide thickness are not sufficient to explain the differences in leakage current between the samples (see Eq. 1).

The open circuit potentials following immersion in aerated 0.05 M K_2SO_4 were also measured for these same three different oxide layers, see Fig. 3. The deposited oxide exhibits the highest open circuit potential, while the O_2-formed oxide exhibits the lowest. This trend, in which the most conductive oxide exhibits the lowest open circuit potential and vice versa, is expected if electron transport across the oxide layer is rate-limiting for the Al oxidation reaction. Recognizing that the measured open circuit potential is determined by the potential at which the anodic current due to Al oxidation is equal and

opposite to the cathodic curent due to $O_{2(aq)}$ reduction (which is the dominant reduction reaction in this aerated solution), a reduction in the anodic current (due to inhibition of electron transport) would require a lower cathodic current to achieve a net current of zero. This requires the potential to rise towards the reversible potential of the $O_{2(aq)}$ reduction reaction. In the limit in which the oxide permits no electron transport (e.g. a very thick oxide layer), the potential should rise up to this limit of the reversible potential of the $O_{2(aq)}$ reduction reaction. Alternatively, in the limit that the oxide provides no barrier to electron transport (e.g. an oxide of zero thickness), the potential should decrease to the value of the reversible potential of the Al oxidation reaction. For an oxide with conductivity between these two extremes, the potential will fall between the two extremes of the reversible potentials of the anodic and cathodic reactions. This present work shows that it should be possible to predict the open circuit potential for a specific oxide on the basis of the measured value of the oxide solid state (i.e. electronic) conductivity. Moreover, changes in the open circuit potential with time (see Fig. 3) may indicate that the electronic conductivity of the oxide is also changing with time due to immersion in the electrolyte. In fact, this is what actually occurs, as is discussed in the next section.

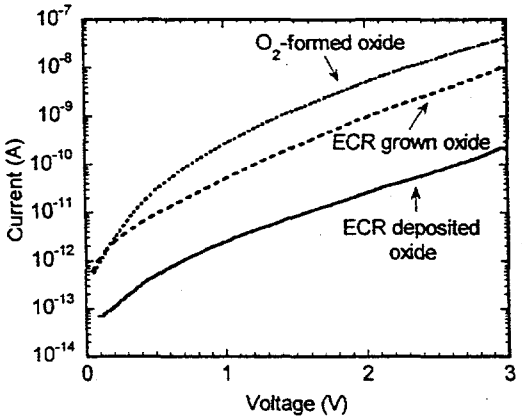

Fig. 2. Current-voltage characteristics for three different Al oxides on Al. The O_2-formed oxide has the highest conductivity and highest electronic defect density.

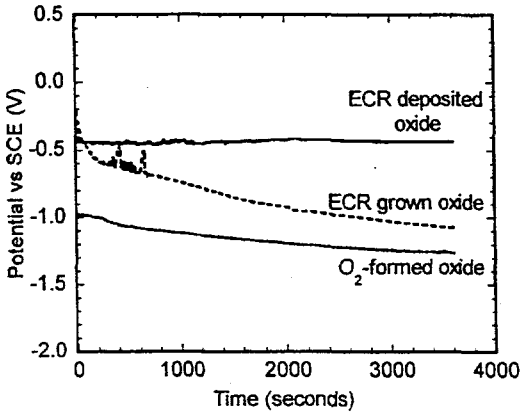

Fig. 3. Open circuit potentials as a function of immersion time in aerated 0.05 M K_2SO_4 solution. The O_2-formed oxide exhibits the lowest open circuit potential.

Effects of Electrochemical Polarization

As we have shown in earlier work, immersion of an Al oxide layer on Al in H_2O (specifically, deionized and deaerated H_2O), leads to a large increase in leakage current (conductivity) of the Al oxide (1). This increase in oxide conductivity occurs even for oxides that are thicker (e.g. 24 nm thick) than the naturally-occurring oxides and which exhibit little apparent change in oxide structure (aside from a slight thinning), as determined by x-ray reflectivity and solid state impedance measurements. In other words, the change in oxide conductivity does not seem to be due to a complete conversion in the structure or phase of the oxide, for example conversion of the entire layer of Al_2O_3 into boehmite, but rather to a change in the nature or concentration of electronic defects within the oxide layer. Using elastic recoil detection for hydrogen, we

discovered that immersion of the Al samples in H_2O leads to hydrogenation of the Al oxide layer: the H content of the oxide layer can be increased by a few at. % (1). These changes in H content of the layers have also been confirmed by secondary ion mass spectroscopy (SIMS) analysis prior to and following H_2O immersion (3). There is also theoretical evidence that Al oxide, specifically the γ-Al_2O_3 phase, lowers its total energy by incorporation of H within the structure up to a maximum of about 7 at. % (4). (It should be noted that the amorphous oxide that spontaneously forms on Al is considered to be structurally closest to the γ-Al_2O_3 phase.) Furthermore, other theoretical evidence suggests that the surface of Al oxide, α-Al_2O_3 in this case, can catalytically dissociate H_2O molecules, liberating atomic H (which, in the case of α-Al_2O_3, combines with a surface O, creating a surface hydroxyl) (5). Considering the experimental evidence alone, it can be concluded that exposure of an Al oxide layer on Al to H_2O leads to an increase in H content of the layer, whether this increase is driven by total energy minimization of the oxide or by the presence of an electrostatic field in the oxide (as is discussed below) is not known at present. Experimentally, it also appears that the increase in H content of the layer is associated with an increase in electrical conductivity of the oxide. Whether this is due to the formation of an electronic defect in the oxide band gap that is associated with a particular H structure or whether H in the oxide layer donates an electron which fills an electronic trap state associated with a different, non-H-related defect is not known.

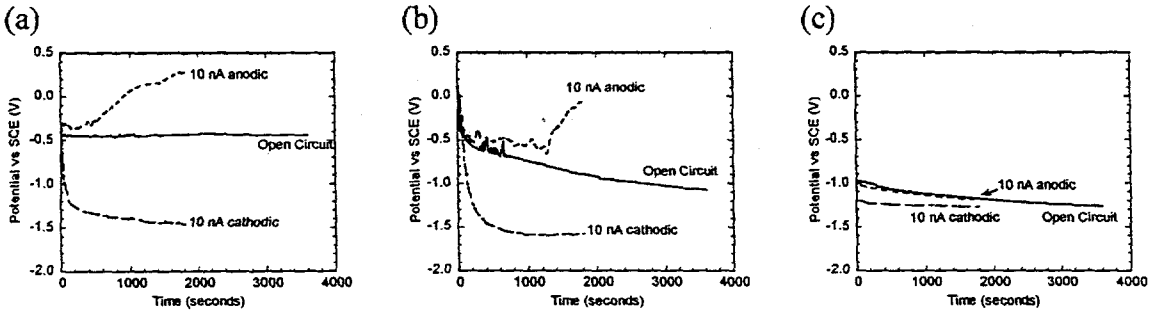

Fig. 4. Potential vs. time for (a) an ECR deposited Al oxide layer, (b) an ECR grown Al oxide layer, and (c) an O_2-formed Al oxide layer (all on Al). Samples were immersed in aerated 0.05 M K_2SO_4 and held at open circuit, 10 nA cathodic current, or 10 nA anodic current.

As noted above, the simplest electrochemical treatment (immersion in H_2O at open circuit) leads to a significant increase in oxide conductivity. Additional changes in the oxide electronic defect density and conductivity occur following anodic and cathodic polarization. For each of the three types of oxides, the samples were held at an anodic current of 10 nA, a cathodic current of 10 nA, or zero current (open circuit) while the electrochemical potential was monitored (each electrochemical treatment was performed on a separate piece of sample from a larger, complete sample). The magnitude of the current was chosen such that there would be negligible oxide growth following 30 min. of applied current. The potential vs. time for the three oxides is shown in Fig. 4. For the ECR deposited and grown oxides, there is a large potential change between anodic and cathodic galvanostatic holds, indicative of the higher polarizability of these less conductive oxides. Following the electrochemical treatments, the oxide conductivity was measured, and these results are shown in Fig. 5. It should be noted that both open circuit and cathodic polarization led to an increase in oxide conductivity, while the anodic

polarization actually decreased the oxide conductivity with respect to the as-grown samples. These results are true for the ECR grown and deposited sample, but not for the O_2-formed sample, which shows similar conductivities for each electrochemical treatment (although the as-grown measurement shows slightly higher conductivity). This result indicates that it is the magnitude of the potential that is important for modifying the oxide conductivity, not the amount of charge passed. For the O_2-formed sample, the potential vs. time for the three electrochemical treatments was almost identical (indicative of the low polarizability of this oxide). Solid state impedance measurements were also performed for all of the samples, and it was found that the oxide capacitance showed no or negligible change as a result of electrochemical treatment, indicating that the apparent changes in oxide conductivity are not due to changes in oxide thickness (i.e. substantial thickening under anodic current or thinning under open circuit and cathodic current). The lack of oxide growth under the applied anodic current is not surprising given that the maximum potential the sample reached is well below the oxide formation field for anodic growth (about 7 MV/cm) (6).

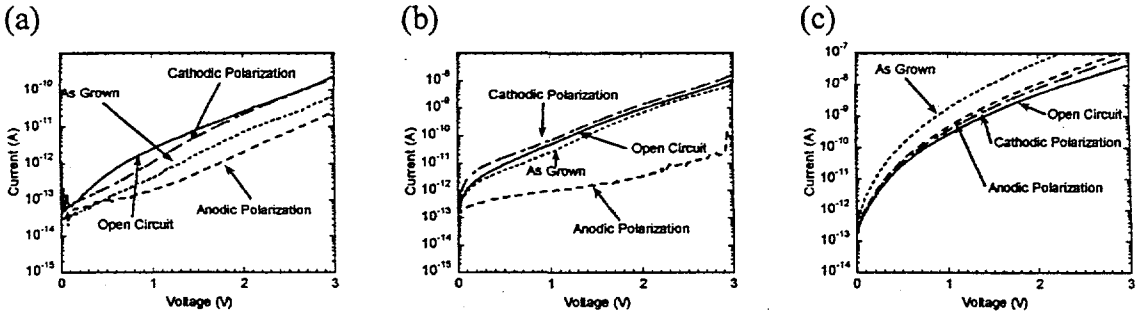

Fig. 5. Current voltage characteristics for (a) an ECR deposited Al oxide layer, (b) an ECR grown Al oxide layer, and (c) an O_2-formed Al oxide layer (all on Al). Electrical measurements were performed prior to (= as grown) and after samples were immersed in aerated 0.05 M K_2SO_4 and held at open circuit, 10 nA cathodic current, or 10 nA anodic current.

The combined solid state and electrochemical measurements suggest that the change in oxide conductivity is due to a change in the concentration or nature of the electronic defects in the oxide layer. In particular, the reduction in conductivity following anodic polarization suggests the presence of a positively charged ionic defect in the oxide that is possibly swept out of the oxide under anodic polarization (positive potential on the Al). Anodic fields applied in the solid state electrical test samples (MIM structures) led to no change in conductivity of the oxide following polarization, which indicates that the positively charged defect does not arise from an electronic defect, such as a trapped hole. (The solid state samples are blocking to ion motion under DC bias, so a positively charged ionic defect would not be swept out of the sample under anodic polarization.) An intriguing possibility is that the charged, mobile defect is associated with protons within the oxide layer. Experiments which would confirm this by looking at the hydrogen content of the layer prior to and following the anodic polarization are not yet complete.

Summarizing the solid state and electrochemical results, these measurements suggest that the open circuit potential of Al is predictable based on solid state

characterization of the oxide conductivity, but the conductivity of the oxide layer changes over time as a result of electrochemical treatment, even treatments as simple as immersion in H_2O at open circuit. In the case of H_2O immersion, the increase in conductivity is found to be associated with H ingress into the oxide film. Both open circuit immersion and cathodic polarization increases the oxide conductivity, while anodic polarization reduces the conductivity, suggesting the presence of a mobile, positively charged defect that contributes to the oxide conductivity. The field that exists within the oxide can play an important role in determining the direction of ionic motion within the layer. The next section discusses the potentials that exist at the oxide interfaces and the resulting direction and magnitude of the potential drop across the oxide layer.

Oxide Interface Potentials

The voltage drop across the oxide layer in the solid state MIM structures plays an important role in determining the magnitude of the breakdown voltage as a function of the direction of applied bias across the structure. Fig. 6 shows the current-voltage characteristics for an Al oxide layer up to the point of breakdown for both positive and negative applied bias (measured with respect to the top contact – positive bias indicating a positive voltage applied to the top contact and a negative bias to the Al layer beneath the oxide). Due to the destructive nature of the test (dielectric breakdown leads to a permanent dead short across the oxide), different contacts are used for each current-voltage scan. The difference between Figs. 6 (a) and (b) is that the device structure in (a) is symmetric, meaning the sample consists only of Al/Al oxide interfaces. In (b), the device is asymmetric, the bottom interface being Al/Al oxide and the top interface being Al oxide/Au. Equilibration of electron chemical potentials between the Al and Au phases leads to charge transfer across the oxide and the formation of a potential drop across the oxide. This potential drop is predictable. For the situation in which there is no interaction between the metal and overlayer, the interface dipole at the surface of the metal is very close to the magnitude of the surface dipole for the metal in vacuum. This dipole leads to a potential difference for electrons at the Fermi level just inside the metal and the vacuum level, and this difference is equal to the work function of the metal. As the interaction between metal and overlayer is increased, the interface dipole deviates significantly from the work function. In the case of metals on Al oxide, recent theoretical evidence by Bogicevic and Jennison suggests that there is little charge transfer between most metals and Al oxide, once the metal layer is more than a few monolayers thick (7). This suggests that the metal work function may provide a good estimate for the interface dipole. For the symmetric interface, no potential drop should exist across the oxide, and positive and negative bias should give the same result for the breakdown voltage of the oxide. This is not true for the asymmetric MIM structure. Using averaged values for the work functions of polycrystalline Al (about 4.2 eV) and Au (about 5.1 eV) (8), we obtain an estimated potential drop across the oxide of 0.9 V. The direction of positive electric field is from the Al towards the Au, i.e. a positively-charged carrier would drift towards the Au interface.

The actual observed potential drop across the oxide may be measured by comparing the breakdown voltage for the symmetric and asymmetric MIM structures. Table I lists the median breakdown voltages for the three types of oxides for both the symmetric and asymmetric MIM structures. For the asymmetric structures, the

breakdown voltage is much higher for positive biases than for negative biases. This asymmetry is due to the fact that the oxide has a built-in voltage across it that behaves as though it were biased negatively even at zero applied bias. Applying a slight positive bias to the top Au contact leads to flat band of the Al oxide. Applying greater positive bias eventually leads to dielectric breakdown of the oxide once a critical field strength is reached [about 8 MV/cm (1)]. Using all of the data from the table, the best estimate for the actual voltage drop across the oxide layer is 1.2 V, which is reasonably close to the estimate of 0.9 V predicted from the difference in metal work functions. For the Al – Au MIM structure, it is necessary to apply greater than 1.2 V of positive bias to the top Au contact before the field in the oxide is reversed.

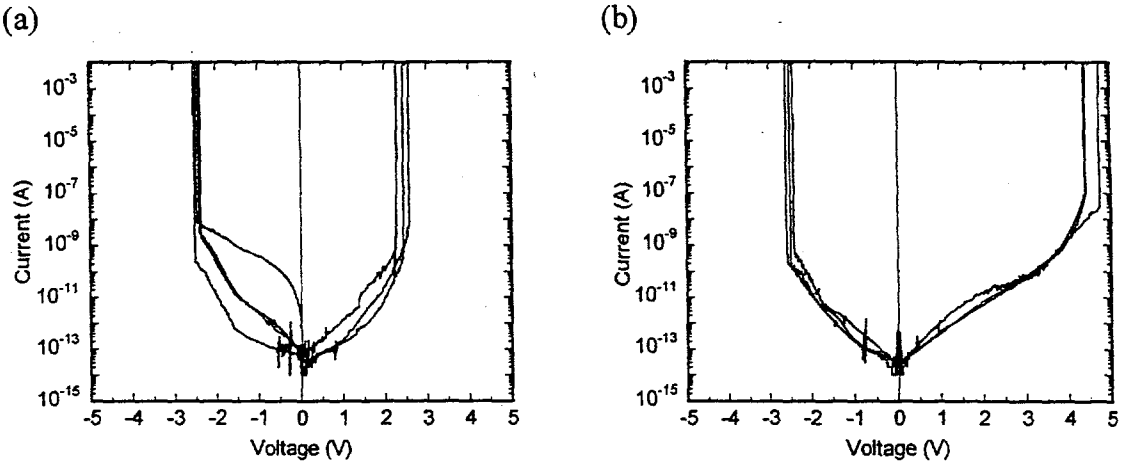

Fig. 6. Current-voltage characteristics for (a) an Al/ECR deposited oxide/Al symmetric MIM structure and (b) an Au/ECR deposited oxide/Al asymmetric MIM structure. The magnitude of the breakdown potential is equal for positive and negative bias in the symmetric structure, but it is unequal in the asymmetric structure.

Table I. Median Breakdown Potentials for Symmetric and Asymmetric MIM Structures

O_2-formed Al oxide	Al/oxide/Al MIM structure		Au/oxide/Al MIM structure	
	-1.70 V	1.77 V	-1.44 V	4.18 V
ECR grown Al oxide	Al/oxide/Al MIM structure		Au/oxide/Al MIM structure	
	-3.62 V	3.48 V	-2.04 V	4.22 V
ECR deposited Al oxide	Al/oxide/Al MIM structure		Au/oxide/Al MIM structure	
	-2.46 V	2.44 V	-2.51 V	4.52 V

It is of great interest to estimate the magnitude of the potential drop across the oxide layer for an Al sample placed in solution. The interface potentials in this situation are much more complicated than the solid state case, however. Let us consider an Al sample immersed in an aqueous solution that contains sufficient ionic strength but no anions which exhibit strong specific adsorption. The 0.05 M K_2SO_4 solution used in the above electrochemical testing is a good model for this system. The voltage drop across the oxide layer will be determined by at least four factors: 1) equilibration of the electron chemical potential in the Al metal and electrolyte solution, 2) the dipole layer at the

oxide/electrolyte interface due to the compact water layer, 3) the dipole layer at the oxide/electrolyte interface due to surface charging of the oxide, and 4) bond dipoles due to hydroxide formation at the oxide/electrolyte interface. The first term sets the total potential drop across the oxide plus oxide/electrolyte interfaces and can be estimated in a similar manner to the solid state case. Using the vacuum level as a reference, the potential difference between the vacuum level and electron chemical potential in the Al at the oxide interface can be assumed to be close to the work function of the Al, which is approximately 4.2 eV (8). The electron chemical potential at the solution side of the oxide interface can be determined from the measured open circuit potential for the sample and knowledge of the effective electron chemical potential for the reversible redox reaction of the reference electrode. Because the solution resistance is low compared to the oxide resistance, we assume that there is negligible potential drop across the solution, so that all of the potential drop occurs across the oxide and the oxide/electrolyte interface. For the O_2-formed and ECR grown oxides, the open circuit potential in aerated 0.05 M K_2SO_4 was approximately –1.0 V vs. the standard calomel electrode (SCE). The potential of the SCE referenced to the normal hydrogen electrode (NHE) is about 0.241 V. The effective electron chemical potential of the NHE with respect to the vacuum level is approximately 4.5 V (i.e. 4.5 V *below* the vacuum level) (9). This establishes the level of the electron chemical potential in solution with respect to the vacuum level = 4.5 V + 0.241 V –1.0 V ≈ 3.7 V. The total potential drop across the oxide and oxide/electrolyte interface is then 4.2 V – 3.7 V ≈ 0.5 V (with the direction of positive electric field going from the solution side towards the Al side, i.e. a positive charge would drift towards the Al). Since the potential drop exists across both the oxide and oxide/electrolyte interface, it is necessary to estimate the potential drop at the oxide/electrolyte interface in order to determine the potential drop across the oxide alone.

The first interfacial potential term to consider is the dipole drop due to the compact water layer at the interface. For a hydrophilic surface, the water layer immediately adjacent to the surface is highly oriented and partially ordered, giving rise to a net dipole moment. The voltage drop across this layer tends to saturate at 0.4 V for hydrophilic surfaces (10). The direction of positive field within this dipole layer is from the solution side towards the Al side. In addition to the compact water layer, there is an additional dipole layer at the oxide/electrolyte interface that is due to charging of the oxide surface. The pH of the aerated 0.05 M K_2SO_4 solution was measured to be close to 6.7. This is below the isoelectronic point of Al oxide on Al which occurs at a pH of about 9.5 (11). As a result, there should be net protonation of the hydroxide groups at the oxide/electrolyte interface, leading to a net positive surface charge. This net positive charge is balanced by a net anionic charge situated at the outer Helmholtz plane, thus establishing a dipole layer. The potential drop across this dipole layer can be estimated to be 59 mV/pH (12). For a pH differential of 3 between the actual solution pH and the pH of the isoelectronic point, a potential drop of about 0.18 V would be expected across this surface dipole layer (in this case, the direction of positive field would be from the Al side towards the solution side). The last term to consider is the bond dipole due to the formation of hydroxyls at the oxide/solution interface. Hydroxyl formation could change the surface dipole of the oxide with the magnitude of the dipole being dependent upon the net orientation of the bond dipole and the magnitude of charge transferred across the O-H bond. Without knowledge of the structure of this interface, it is difficult to estimate the magnitude of this dipole term, but we can resort to solid state measurements for an estimate. For the symmetric MIM structures that consist of Al at both oxide interfaces,

tests were made in which the surface of the oxide was exposed to H_2O prior to evaporation of the top Al contact. If the surface hydroxide groups survived the Al deposition step, we would expect that any significant net dipole for these hydroxyl groups would still be present at the top Al/Al oxide interface. This would introduce a potential drop at this interface, which would break the symmetry of the MIM structure. If the magnitude of this change were significant, we would expect a different breakdown potential for forward biasing of the MIM structure compared to negative biasing of the structure (similar to what is seen in the asymmetric MIM structure). No significant difference was seen between positive and negative biasing, however, suggesting that the magnitude of this hydroxyl bond dipole is not large. We, therefore, assume it to be zero.

Summing all terms that contribute to the potential drop across the oxide layer in solution, we obtain 0.5 V – 0.4 V + 0.18 V + 0 V = 0.3 V. This estimate indicates that at open circuit there should be about 0.3 V dropped across the oxide layer with the direction of positive electric field being from the solution side to the Al side. A schematic of the potential drop is shown in Fig. 7. The built-in potential drop is important, because it is in the same direction as the potential drop that would exist for cathodically polarizing the sample (negative potential on the Al). Positively charged species (protons, for example) within the oxide would be attracted by the built-in field towards the Al/oxide interface under both open circuit and cathodic polarization. Hence there would be an electrostatic driving force for H ingress into the sample independent of any thermodynamic driving force. Note that it would be necessary to apply greater than 0.3 V (with respect to the open circuit potential) of anodic polarization to the sample in order to reverse the field direction so that positively-charged species would be expelled from the oxide layer. It should also be noted that the oxide is relatively far from the field necessary for dielectric breakdown when immersed in non-aggressive electrolytes (for a 4.5 nm thick oxide, an anodic potential of ~ 3.4 V with respect to open circuit would be necessary to achieve dielectric breakdown).

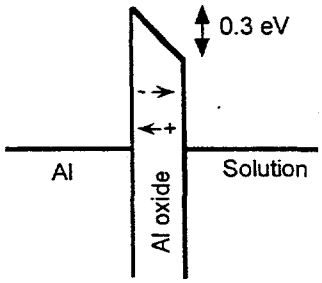

Fig. 7. Energy band diagram of the potential drop across the Al oxide layer when immersed in solution at open circuit. The lines represent the electron chemical potential level within the Al and solution. The field in the oxide would attract positive charge towards the Al interface. (The alignment between the electron chemical potential levels and the conduction band of the Al oxide is not meant to be accurate.)

All of the above discussion is for an oxide immersed in a non-aggressive electrolyte (one which contains anions that do not exhibit strong contact adsorption). For aggressive electrolytes, such as Cl^--containing electrolytes, the situation can be much different. Specific adsorption of Cl^- anions at the oxide electrolyte interface introduces another dipole layer term at the oxide/electrolyte interface. Assuming the open circuit potential does not change when Cl^- is added to the solution, specific adsorption of one quarter of a monolayer of Cl^- at the oxide/electrolyte interface would be sufficient to reverse the 0.3 V potential drop across the oxide, reversing the field direction from one that is characteristic of cathodic polarization to one that is characteristics of anodic polarization. The effects of Cl^- exposure on the electrical properties and field across the oxide layer is currently being investigated.

CONCLUSIONS

Combined solid state and electrochemical measurements revealed (1) that the measured open circuit potential of the oxide on Al in a non-aggressive (e.g. SO_4^{2-}-based) electrolyte is inversely correlated with the oxide electronic defect density (viz., lower oxide conductivities are correlated with higher open circuit potentials), and (2) the electronic defect density within the Al oxide is increased upon exposure to an aqueous electrolyte at open circuit or applied cathodic potentials, while the electronic defect density is reduced upon exposure to slight anodic potentials in solution. This last result, combined with recent theoretical predictions, suggests that hydrogen may be associated with electronic defects within the Al oxide, and that this H may be a mobile species, diffusing as H^+. The potential drop across the oxide layer when immersed in solution at open circuit conditions was also estimated and found to be 0.3 V. This gives a built-in field in the oxide that would attract positive charge towards the Al/oxide interface under open circuit and cathodic polarization. Anodic polarization above 0.3 V, with respect to the open circuit potential, would reverse this built-in field direction.

ACKNOWLEDGMENTS

Valuable discussions with B. Bunker, K. Zavadil, K. Sohlberg, D. Jennison, A. Bogicevic, and H. Isaacs are gratefully acknowledged. This work was supported by the DOE Office of Basic Energy Sciences (BES). Sandia is a multiprogram laboratory operated by Sandia Corp., a Lockheed Martin Co., under U.S. DOE contract DE-AC04-94AL85000.

REFERENCES

1. J. P. Sullivan, J. C. Barbour, R. G. Dunn, K.-A. Son, L. P. Montes, N. Missert, and R. G. Copeland, in *Critical Factors in Localized Corrosion III*, R. G. Kelly, G. S. Frankel, P. M. Natishan, and R. C. Newman, Editors, PV 98-17, p. 111, The Electrochemical Society Proceedings Series, Pennington, NJ (1999).
2. S. M. Sze, *Physics of Semiconductor Devices*, John Wiley and Sons, New York (1981).

3. B. Bunker, G. Nelson, F. D. Wall, J. C. Barbour, J. P. Sullivan, C. Wendisch, M. Engelhard, D. Baer, and J. Hren, *2000 Spring Meeting of the Materials Research Society*, April 25, 2000 (unpublished).
4. K. Sohlberg, S. J. Pennycook, and S. T. Pantelides, J. Am. Chem. Soc., **121**, 7493 (1999).
5. K. C. Hass, W. F. Schneider, A. Curioni, and W. Andreoni, Science, **282**, 265 (1998).
6. M. M. Lohrengel, Mat. Sci. Eng., **R11**, 243 (1993).
7. A. Bogicevic and D. R. Jennison, Phys. Rev. Lett., **82**, 4050 (1999).
8. *CRC Handbook of Chemistry and Physics*, R. C. Weast, Editor, p. E-78, CRC Press, Boca Raton, Florida (1988).
9. N. Sato, *Electrochemistry at Metal and Semiconductor Electrodes*, p. 57, Elsevier, Amsterdam (1998).
10. S. Trasatti, *Modern Aspects of Electrochemistry, No. 13*, p. 81, Plenum Press, New York (1979).
11. E. McCafferty, in *Critical Factors in Localized Corrosion III*, R. G. Kelly, G. S. Frankel, P. M. Natishan, and R. C. Newman, Editors, PV 98-17, p. 42, The Electrochemical Society Proceedings Series, Pennington, NJ (1999).
12. N. Sato, *Electrochemistry at Metal and Semiconductor Electrodes*, p. 183, Elsevier, Amsterdam (1998).